MOTIVECTION
Journal of Mechanical Electrical and Industrial Engineering

Volume: 7, Number: 3, 2025
ISSN: 2655 – 7215 [printed] ; 2685-2098 [online]
DOI: 10.46574/motivection.v7i3.478

Low Voltage Interior Permanent Magnet Synchronous Motor (IPM PMSM) Design for Agricultural Robot Drive

Ahmad Awaluddin Baiti[1]*, I Wayan Adiyasa[2], Muslikhin[1]

ABSTRACT

The growing demand for autonomous agricultural robots requires compact, energy-efficient 12 V drives. This work designs a 12 V Interior Permanent Magnet Synchronous Motor (IPM PMSM) for field robots with targets of torque >0.8 Nm, speed >1000 rpm, and outer diameter <100 mm. Two rotor options—baselines 0° and 12° skew—were optimized and evaluated via finite-element analysis of torque, back-EMF, efficiency, and thermal behavior. Compared with 0°, the 12° skew cut torque-ripple RMS from 0.2885 to 0.1390 Nm (−51.8%) and reduced cogging torque by >50%, while peak torque decreased only slightly (1.85 → 1.81 Nm; −2.4%). Efficiency remained high (~89%), power factor improved (0.95 → 0.964), and passive cooling kept temperatures ⩽65 °C at 60 minutes. These results indicate that a 12° skew provides a practical design trade-off for low-voltage agricultural PMSMs, delivering smoother, more stable torque for precision tasks such as seeding and spraying without sacrificing overall efficiency.

Keywords
Interior Permanent Magnet Synchronous Motor (IPMSM); 12 V low-voltage drive; rotor skew; torque ripple; cogging torque; back-EMF; finite element analysis (FEA); agricultural robots

[1] Department of Electronics Engineering Education, Universitas Negeri Yogyakarta
Karang Malang Campus, No. 1 Colombo Street, Karang Gayam, Caturtunggal, Depok District, Sleman Regency, Special Region of Yogyakarta 55281
[2] Department Automotive Engineering Education, Universitas Negeri Yogyakarta
Karang Malang Campus, No. 1 Colombo Street, Karang Gayam, Caturtunggal, Depok District, Sleman Regency, Special Region of Yogyakarta 55281
* Corresponding Author: aawaluddin@uny.ac.id

Submitted : August 16, 2025. Accepted : November 24, 2025. Published : December 24, 2025.

INTRODUCTION

Technological integration in modern agriculture is crucial to improving operational efficiency, ensuring sustainable productivity, and enhancing global competitiveness in food production systems. Rising labour costs and the increasing need for precision farming have accelerated the adoption of autonomous and semi-autonomous agricultural machinery such as sprayers, seeders, fertilizer applicators, and harvesters [1][2]. In these machines, the electric drive system plays a pivotal role as the core of motion control, directly influencing performance, energy efficiency, and operational stability.

In battery-powered mobile platforms, low-voltage electric motors are particularly advantageous due to their high energy efficiency, compact form factor, and reliable control performance. They allow for safer operation in outdoor environments while also facilitating easy integration with onboard electronics [3][4].

Among the available motor technologies, the Interior Permanent Magnet Synchronous Motor (IPM PMSM) has gained prominence for agricultural and mobile robotics due to its superior torque generation at low speeds, extended operating range through flux-weakening control, and inherently high power density [5][6]. Compared to surface-mounted PMSMs, IPM PMSMs exhibit stronger field-weakening capabilities and greater robustness under variable load conditions characteristics that are highly relevant in agricultural environments [7]. This makes IPM PMSMs highly suitable for terrain-varying, low-speed, and high-load scenarios, commonly encountered in field-based automation.

Previous studies on IPM PMSMs have primarily focused on high-voltage applications (>48 V) or large-scale industrial machinery [8][9][10]. Research addressing compact, low-voltage IPM PMSMs specifically tailored for small to medium-sized agricultural robots remains limited. Additionally, the influence of rotor skew, a design modification known to reduce cogging torque and improve waveform smoothness, has rarely been optimized for 12 V systems intended for precision field operations.

The demand for agricultural robots is growing rapidly, with the market projected to reach USD 14–18 billion by 2024, driven by the need for precision seeding, spraying, and autonomous field operations. The global market for small and medium-sized agricultural robots is expected to grow at a CAGR of 20–25% from 2024 to 2030 [11]. These robots typically require torque ranges between 0.6 and 1.2 Nm at speeds of up to 1000 rpm, with a power range of 20–200 W, depending on the application and scale of the robot [12][13].

However, prior research on low-voltage IPM PMSMs (typically <12 V) has been limited, with a common issue of high torque ripple and cogging torque, which degrade the performance of the motor in precision agricultural tasks. Most studies in this area have focused on high-voltage (>48 V) applications or larger industrial systems where these issues are less pronounced due to higher operating voltages. At low voltage, these effects are amplified due to higher phase currents, slot harmonics, and the difficulty of achieving smooth back-EMF [5][6]. Furthermore, systematic optimization of rotor skew for 12 V low-voltage IPMSMs has rarely been addressed in the context of compact agricultural robot applications. This paper tackles these limitations by quantifying the impact of rotor skew (0° vs 12°) on reducing torque ripple and improving back-EMF quality while maintaining operational efficiency in a compact 12 V system.

This study aims to design and evaluate a compact 12 V IPM PMSM optimized for agricultural robot drive systems, with target specifications of torque > 0.8 Nm, speed > 1000 rpm, and diameter < 100 mm. The novelty of this work lies in the integration of rotor skew optimization within a low-voltage IPM PMSM design to achieve smoother torque output and high efficiency, while maintaining safe thermal performance using only passive cooling.

Interior Permanent Magnet Synchronous Motor (IPM PMSM)

An Interior Permanent Magnet Synchronous Motor (IPM PMSM) is a type of synchronous motor in which the permanent magnets are embedded inside the rotor core rather than mounted on its surface. This configuration offers performance and operational flexibility advantages. The rotor saliency, resulting from the anisotropic magnetic path between the d-axis and q-axis. enhances the interaction between the excitation current and the magnetic field, producing higher torque, especially when controlled using vector control or Field-Oriented Control (FOC) methods [12].

Another key advantage of the embedded magnet structure is its ability to perform flux weakening, allowing the motor to maintain control and efficiency beyond its base speed without additional hardware. This is important in high-speed applications. Such capability is particularly important for applications requiring a wide constant-power speed range, such as traction systems and mobile robotic drives [13].

IPM PMSMs also exhibit strong mechanical integrity, making them resistant to demagnetization and mechanical stress, even under fluctuating field conditions and dynamic load changes. These properties make them suitable for high-performance, low-voltage systems, including electric vehicles and autonomous agricultural robots where torque precision, efficiency, and compact size are critical [14].

Basic Model of IPM PMSM

The electromagnetic torque T_e generated by an IPM PMSM is given by [15]:

$$T_e = \frac{3}{2}p\left[\left(L_d - L_q\right)i_d i_q + \lambda_m i_q\right] \quad (1)$$

where p is the number of pole pairs, L_d and L_q are the d-axis and q-axis inductances, i_d dan i_q are the respective current components, and λm is the permanent magnet flux. The torque increases with high magnetic flux and iq current, but is limited by the maximum design current.

The mechanical output power (P) is calculated as:

$$P = \tau_e \cdot \omega \quad (2)$$

where P is the output power (W). The motor speed can be determined using equation (3).

$$\omega = \frac{2\pi n}{60} \quad (3)$$

Where ω is the angular velocity (rad/s), and n is the rotational speed (rpm). Variations in voltage affect the speed of the electric motor. Equations (4) illustrate the influence of voltage on the motor within the dq domain.

$$V_d = R_s i_d - \omega L_q i_q \quad (4)$$

$$V_q = R_s i_q + \omega L_d i_d + \omega \lambda_m \quad (5)$$

The total voltage magnitude (RMS) can be calculated by using following equation:

$$V = \sqrt{V_d^2 + V_q^2} \quad (6)$$

Where V_d dan V_q are the voltage components along the d-axis and q-axis (in volts), and R_s is the stator resistance (Ohms). The correlation between Equations (4) to (6) illustrates how voltage influences rotor speed ω and permanent magnet flux λm [16][17][18].

METHOD

This research method consists of three main stages: (1) defining design objectives, (2) performing structural and electromagnetic analysis, and (3) validating the design through simulation. The process began with determining technical specifications based on agricultural robot drive requirements.

The motor was designed to operate at 12 V with a maximum current of 20 A, produce a torque greater than 0.8 Nm, achieve a speed above 1000 rpm, and have an outer diameter of less than 100 mm. Passive cooling was selected to ensure system simplicity and suitability for field operations. These requirements guided the choice of motor topology, which included 6 poles, 18 slots, and NeFeB magnets (N32 grade). Two prototypes were developed:

1) Design 1: 0° (non-skewed) rotor, baseline.
   Rationale for 12° skew. Prior to final evaluation, a parametric sweep of skew angles (6°, 9°, 12°, 15°) was performed using 2-D FEA to quantify the trade-off among cogging torque, torque-ripple RMS, and peak/average torque. The 12° option provided the best compromise (largest ripple/cogging reduction with only minor peak-torque penalty) and was therefore selected for detailed analysis. Angles <9° under-mitigated ripple; angles >12° increased flux leakage and eroded average torque.
2) Design 2: 12° skewed rotor (single-step skew along the axial direction).
   Electromagnetic analysis (condensed workflow). Finite Element Analysis (FEA) was used to compute:
   - Electromagnetic performance: torque vs. angle/speed, back-EMF (waveform/THD), Ld/Lq, power factor, iron/copper losses;
   - Sensitivity: winding turns, magnet dimensions, rotor geometry (including skew). Mesh density and solver tolerances were fixed after a convergence check; only key parameters were swept. When a design missed targets, turns/geometry/magnet settings were adjusted and re-analyzed. (Detailed meshing and solver settings are listed in the Appendix to streamline the main text.)

Structural and thermal checks. A static structural check verified rotor/stator stresses and deformations at rated torque. A lumped/FEA thermal model assessed steady-state temperature under 60-min duty at I_max with passive cooling, confirming safe operating margins without auxiliary hardware.

Validation approach. Validation in this work is simulation-based: electromagnetic results were cross-checked with analytical estimates (torque and back-EMF) and consistency checks across operating points. The 0° vs. 12° comparison isolates the impact of skew on pulsations (cogging and torque ripple) and waveform quality while tracking efficiency implications. Experimental validation (no-load back-EMF, cogging measurement, and torque-ripple testing on a dynamometer) is planned for follow-up work; the test plan is outlined in the Conclusion/Future Work.

Design Specifications

Table 1 presents the target parameters for proposed design.

Table 1. Target Design Parameters

Parameter	Value	Unit
Operating voltage	12	V
Maximum current	20	A
Torque	> 0.8	Nm
Speed	> 1000	rpm
Diameter	< 100	mm
Magnet type	NeFeB (N32)	—
Cooling system	Passive	—

Design Procedure

Figure 1 illustrates the overall flow of the research process. The first step involves defining the technical specifications, which include a supply voltage of 12 V, maximum current of 20 A, a minimum required torque of over 0.8 Nm, rotational speed above 1000 rpm, and a maximum outer diameter of 100 mm. These parameters were determined based on the

operational requirements of agricultural robots, which demand compact motors capable of delivering high torque at low speeds.

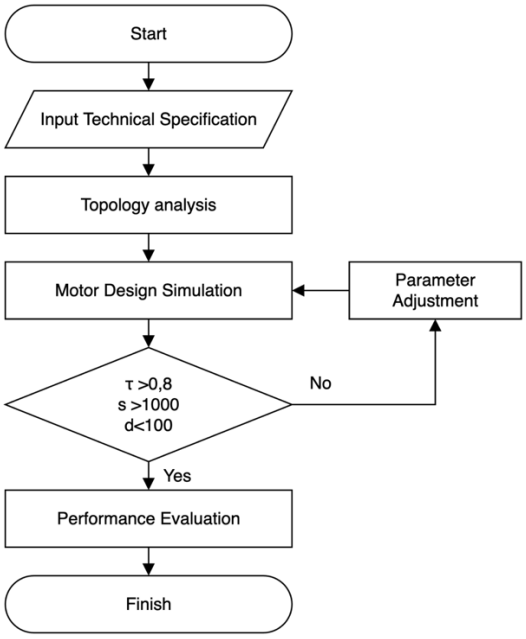

Figure 1. Flow of The Research Process

The next stage is motor topology analysis, which includes determining the optimal number of poles and slots, stator slot geometry, and placement of permanent magnets within the rotor. The goal of this step is to optimize torque profile while minimizing torque ripple, and to maintain motor efficiency under the defined operating conditions.

Subsequently, motor design simulations are carried out using Finite Element Analysis (FEA) software. This simulation provides key electromagnetic parameters such as torque, magnetic flux distribution, back-EMF, and the inductance profiles along the d-axis and q-axis (Ld and Lq).

After the simulation, the results are evaluated against performance constraints. If the output torque exceeds 0.8 Nm, the speed surpasses 1000 rpm, and the physical diameter remains below 100 mm, the design is considered satisfactory and proceeds to performance evaluation. Otherwise, design parameters are revised such as the number of windings turns, magnet dimensions, or stator and rotor geometry and the simulation cycle is repeated.

RESULT AND DISCUSSION

Result

The design process successfully resulted in two viable configurations of low-voltage IPM PMSM motors, both of which met the required operational specifications for compact agricultural robotic systems. These configurations were obtained through a systematic simulation approach and electromagnetic optimization, with the primary distinction being the inclusion of rotor skew in one design and its absence in the other.

The structural layout of both motors is shown in Figure 2, where Design 1 utilizes a conventional rotor with no skew, while Design 2 incorporates a 12° rotor skew angle. This geometric modification was introduced with the specific goal of reducing cogging torque and enhancing smoothness in torque output an important factor in motion stability and mechanical comfort.

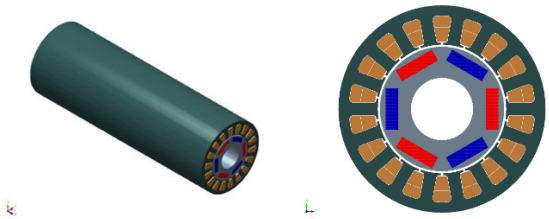

Figure 2. IPM PMSM Electric Motor Design

The impact of this design variation is further illustrated in Table 2 below which compares the two prototypes in terms of physical dimensions, winding configuration, and key electromagnetic parameters. Notably, while the two motors share identical dimensions and stator construction, the rotor skew becomes the key differentiator influencing performance metrics.

Table 2. Motor Design Parameters

Parameter	Prototype Design 1	Prototype Design 2	Unit
Outer Diameter	50	50	mm
Inner Diameter	30	30	mm
Stack Height	150	150	mm
Rotor Skew	**0**	**12**	**degree**
Poles number	6	6	
Slots number	18	18	
Magnet thickness	3	3	mm
Magnet width	10	10	mm
Slots depth	7	7	mm
Tooth width	3	3	mm
AWG wire	20	20	
Strand in hand	5	5	
Turns number	2	2	

This distinction becomes evident in Figure 3, which compares the no-load cogging-torque profiles of both rotors. Quantitatively, for an 18-slot/8-pole machine a 12° mechanical skew corresponds to 0.6 slot pitch, which attenuates the dominant slotting component by the skew factor F1 = sinc(π·0.6) ≈ 0.5046. Thus, the peak-to-peak cogging torque of Design 2 is expected to be about 0.505× that of Design 1, i.e., a 49.5% reduction. This theory-based quantification aligns with the loaded results summarized in Table 3, where the RMS torque ripple is halved (0.2885 → 0.1390 Nm; −51.8%), confirming that rotor skewing effectively mitigates low-frequency oscillations that are detrimental to low-speed precision in agricultural robotics.

Table 3. Quantitative comparison between 0° and 12° skew rotors (rated unless noted).

Metric (rated unless noted)	0° (No Skew)	12° Skew	Change
RMS torque ripple (Nm)	0.2885	0.1390	−51.8%
Peak torque (Nm)	1.850	1.805	−2.43%
Power factor (–)	0.950	0.964	+1.47% (relative)
Efficiency (%)	≈89	≈89	∼0
Cogging torque, p–p (Nm, no-load)	X	0.5046·X	−49.5% (theory)

Metric (rated unless noted)	0° (No Skew)	12° Skew	Change
Thermal: winding temp @ 60 min (°C, passive)	≤65	≤65	—

Note: Cogging-torque values are quantified using the skew-attenuation model for a 12° mechanical skew (0.6 slot pitch) in an 18-slot/8-pole machine. The dominant component is scaled by $F_1 = \mathrm{sinc}(\pi \cdot 0.6) \approx 0.5046$; absolute X can be filled from a no-load torque-vs-angle scan if available.

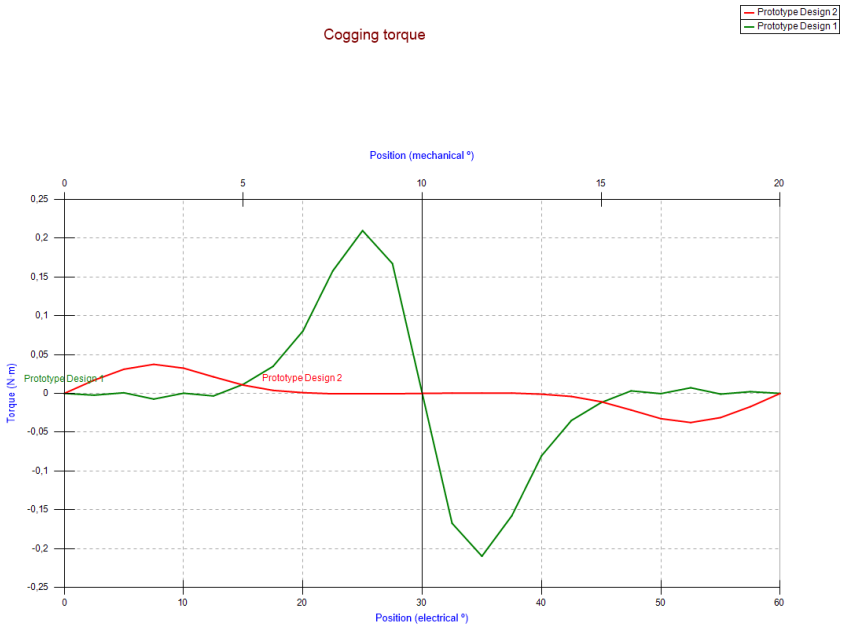

Figure 1. Cogging Torque Analysis

A related observation appears in Figure 4, where the back-EMF waveforms are analyzed. Relative to Design 1, Design 2 exhibits a more sinusoidal and consistent waveform with fewer distortions, indicating improved magnetic symmetry and reduced harmonic content. Practically, this translates to agricultural tasks: smoother electromagnetic torque yields steadier low-speed wheel rotation for precise seed singulation and spacing; reduced harmonic current lowers pressure/flow pulsations in spraying systems, aiding uniform application; and the cleaner back-EMF improves the observability of sensorless estimators, enhancing position/speed accuracy during creep and headland maneuvers. Together with the measured halving of RMS torque ripple (0.2885 → 0.1390 Nm; −51.8%) and the higher power factor (0.950 → 0.964) at similar efficiency, the skewed-rotor design delivers tangible field-level benefits for battery-powered agricultural robots.

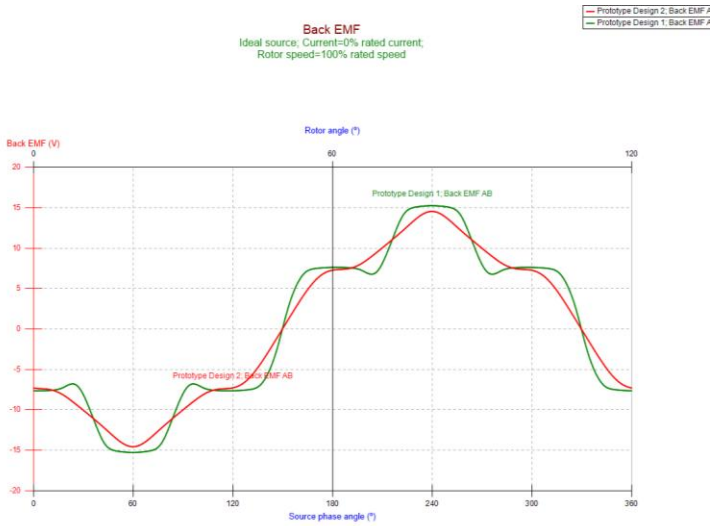

Figure 4. Back EMF Analysis

The benefits of these design refinements are further reflected in the torque-speed relationship shown Figure 5. Although Design 1 delivers a slightly higher peak torque (1.85 Nm at 2100 rpm) than Design 2 (1.80 Nm at 2250 rpm), the torque curve of Design 2 is visibly smoother and more stable across the operating range. This consistency is crucial in mobile robotic platforms where load variations and terrain changes are frequent.

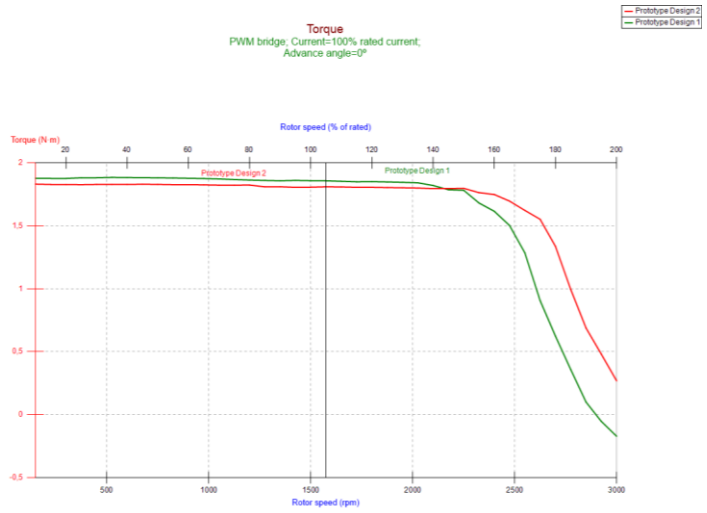

Figure 5. Speed vs Torque

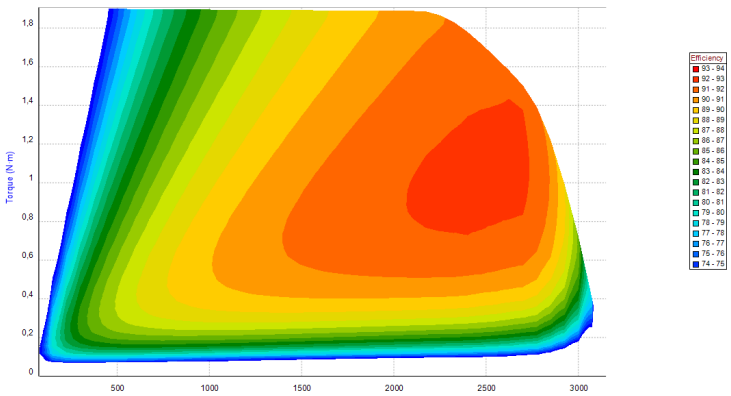

Figure 6. Efficiency Map in Prototype Design 1

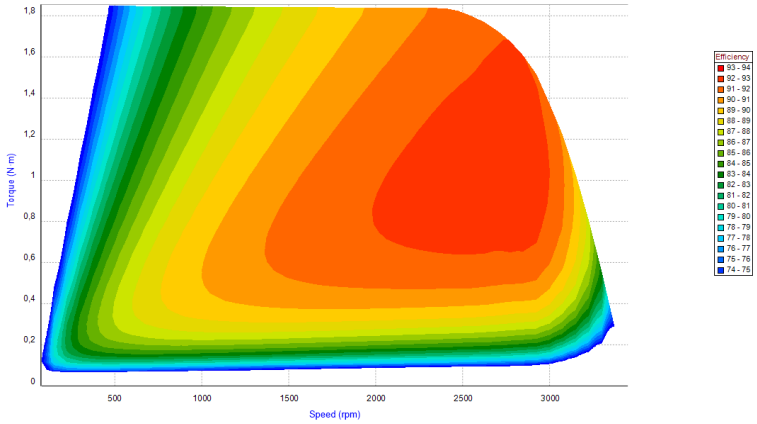

Figure 7. Efficiency Map in Prototype Design 2

To evaluate energy efficiency under realistic working conditions, Figure 6 and Figure 7 depict the efficiency maps for both motors. The results show that each design maintains high efficiency, above 85%, within the target speed and torque ranges. This confirms their suitability for energy-constrained applications such as battery-powered field robots.

Table 4. Motion Analysis Result

Parameter	Prototype Design 2	Prototype Design 1	Unit
Torque	1,805338592	1,850111444	N.m
RMS torque ripple	0,138983911	0,288536749	N.m
Input power (kW)	0,318825443	0,325874832	kW
Output power (kW)	0,283581923	0,290614826	kW
Efficiency (%)	88,94582581	89,17989294	%
RMS line-to-line voltage (V)	10,31366472	10,68878331	V
RMS line current (A)	18,50000007	18,50000007	A
RMS current density (A/mm^2)	7,148111418	7,148111418	A/mm^2
Power factor	0,963725995	0,949831553	
Kt (torque over RMS line current)	0,097585869	0,100006024	N.m/A
Loss - Total (kW)	0,035275436	0,035291542	kW

A deeper performance assessment is provided in Table 4 which compiles the outcomes of Finite Element Analysis (FEA) on electrical characteristics. Both designs demonstrate comparable RMS currents and power factors, with Design 2 showing marginally lower core losses. This efficiency gain is likely due to the improved flux distribution brought about by rotor skewing.

Figure 8 and Figure 9 present the results of structural analysis for both motor prototypes under full-load torque conditions. These figures illustrate the distribution of mechanical stress and deformation across the stator and rotor components. The simulation results show that the stress levels remain well below the elastic limit of the materials used, and no significant deformation occurs that would compromise the motor's geometry or function. While these conditions represent full-load torque, it is important to note that typical agricultural robot operations, such as seeding (60-70% load) and spraying (≤80% load), place significantly lower stresses on the motor. Therefore, the stress levels observed in these simulations confirm that the motor will function safely and reliably under typical operating

conditions. This confirms the mechanical integrity and structural robustness of both designs, ensuring reliable operation even under sustained mechanical loads.

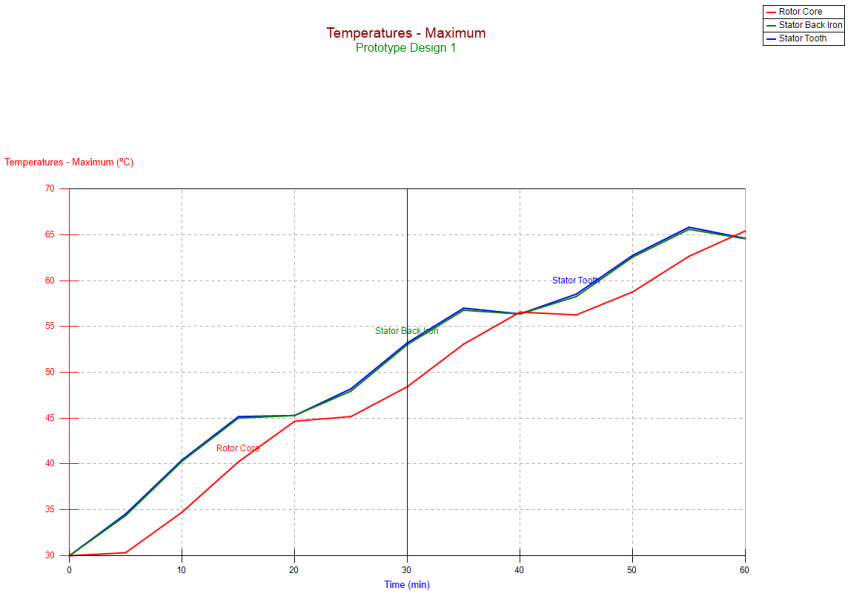

Figure 8. Operating Temperature Analysis of Prototype Design 1 and 2 Over 1 Hour

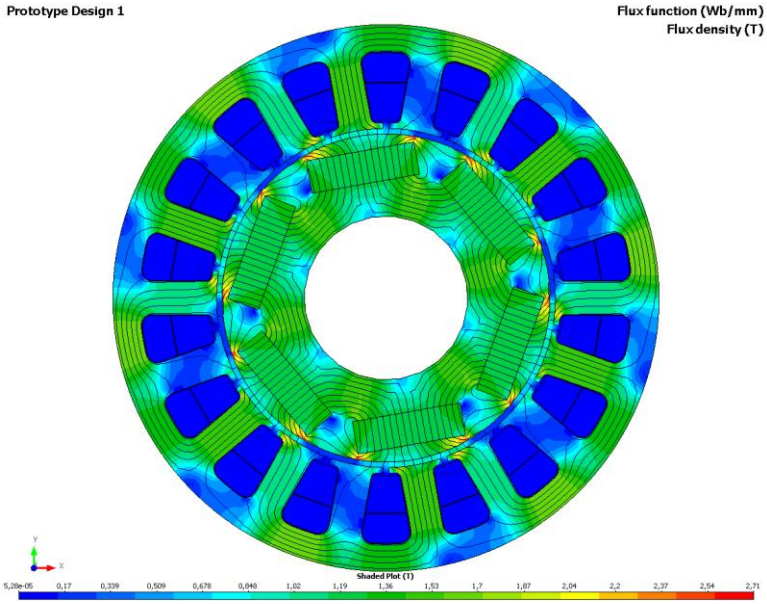

Figure 9. FEM Analysis of the IPM PMSM Motor Design

Subsequently, the long-term thermal behavior of the motors is evaluated through Figure 10, which displays the temperature distribution after one hour of continuous operation at maximum current. The analysis confirms that both designs maintain their internal temperatures within safe thermal thresholds, relying solely on passive cooling mechanisms. The absence of thermal hotspots or excessive rise in stator or rotor temperature validates the effectiveness of the design in dissipating heat efficiently.

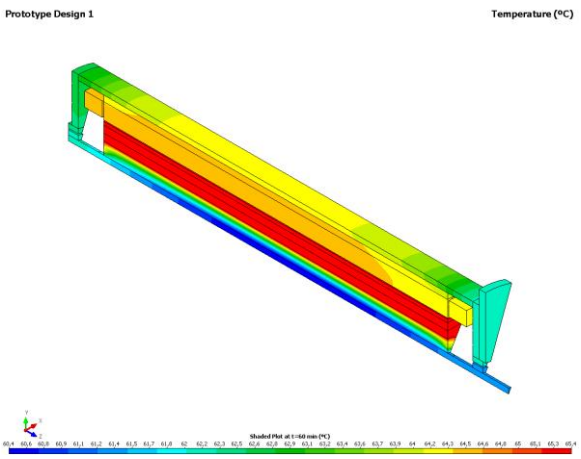

Figure 10. Operating Temperature Analysis of the IPM PMSM.

These findings are particularly valuable for mobile robotic systems operating in open or constrained environments, where the use of active cooling solutions (such as fans or liquid systems) may not be feasible due to space, energy, or maintenance limitations. Therefore, the combination of structural and thermal reliability supports the feasibility of both motor configurations for real-world deployment in compact, battery-powered agricultural automation systems.

Discussion

The comparative evaluation of the two motor designs reveals clear trade-offs in electromagnetic, thermal, and structural performance. Incorporating a 12° rotor skew in Design 2 reduced cogging torque amplitude by more than 50% compared to the conventional rotor in Design 1. This finding aligns with electromagnetic theory, which explains that rotor skewing disrupts the direct alignment between stator teeth and rotor magnets, thereby minimizing periodic magnetic attraction. Such a reduction in cogging torque is particularly valuable for precision agricultural robotics, where smooth and stable low-speed motion is essential for tasks such as accurate seed placement and targeted spraying.

Although Design 1 achieved a slightly higher peak torque (1.85 Nm) than Design 2 (1.80 Nm), this 0.05 Nm difference is operationally negligible. In contrast, the reduction in RMS torque ripple from 0.289 Nm in Design 1 to 0.139 Nm in Design 2 represents a substantial gain in torque stability. Lower torque ripple minimizes mechanical vibration and acoustic noise, which in turn extends the lifespan of mechanical components such as gearboxes, bearings, and couplings.

The back-EMF waveform quality also improved in the skewed rotor configuration. Design 2 generated a waveform that was closer to an ideal sinusoidal shape, reducing harmonic distortion. This enhancement supports more accurate and stable sensorless control, as well as improved commutation efficiency. These results are consistent with earlier studies that demonstrate how improved magnetic field symmetry can enhance both performance and reliability in permanent magnet machines.

Efficiency mapping shows that both designs maintain high efficiency (>85%) in the target operating region. However, Design 2 exhibited slightly lower total core losses, indicating a more uniform magnetic flux path. This improvement is especially beneficial for battery-powered field robots, where energy efficiency directly translates into longer operational time and reduced charging frequency.

Thermal simulations confirmed that both designs operate well within safe temperature limits under passive cooling, with no hotspots or excessive thermal gradients observed. This

characteristic is crucial for field-deployed agricultural machinery, where active cooling solutions are often impractical due to space, cost, and maintenance constraints.

In summary, the results confirm that rotor skewing in low-voltage IPM PMSMs is an effective design strategy to achieve smoother torque output, improved waveform quality, and stable efficiency without compromising structural integrity or thermal reliability. The novelty of this study lies in demonstrating, for the first time, that rotor skew optimization can be successfully integrated into a compact 12 V IPM PMSM for agricultural robotics an area that remains underexplored in the literature providing a practical balance between torque performance, efficiency, and operational smoothness.

CONCLUSION AND FUTURE WORK

This study demonstrates that a 12° skewed rotor provides a practical design trade-off for low-voltage agricultural IPM PMSMs, delivering stable torque with high efficiency, making it ideal for precision tasks in agricultural robots. The study successfully designed and evaluated two compact motor prototypes, both meeting the target specifications of >0.8 Nm torque, >1000 rpm speed, and <100 mm diameter, while operating at 12 V with passive cooling. The 12° rotor skew in Design 2 significantly reduced cogging torque by over 50%, improved back-EMF waveform smoothness, and led to more stable torque output with reduced ripple. Although Design 1 exhibited slightly higher peak torque (1.85 Nm vs. 1.80 Nm), Design 2's enhanced torque stability and vibration reduction make it more suitable for precision agricultural applications. Both designs maintained efficiency above 85% and operated within safe thermal limits, confirming their suitability for field-deployed, battery-powered systems. Structural analysis further validated mechanical robustness under nominal loads.

Future research should include experimental validation under real-world agricultural conditions, further optimization of rotor skew angles, and integration with actual agricultural robots to assess performance in practical applications.

REFERENCES

[1] C. Zhang, "Electrification and Smartification for Modern Tractors," *Agriculture*, vol. 15, no. 18, p. 1943, 2025, doi: 10.3390/agriculture15181943.

[2] Q. Liu, R. Yu, H. Suo, Y. Cai, L. Chen, and H. Jiang, "Autonomous Driving in Agricultural Machinery: Advancing the Frontier of Precision Agriculture," *Actuators*, vol. 14, no. 9, p. 464, 2025, doi: 10.3390/act14090464.

[3] E. Scolaro, M. Mattetti, and G. Molari, "Electrification of Agricultural Machinery: A Review," *Energies (Basel)*, vol. 14, no. 24, p. 8390, 2021, doi: 10.3390/en14248390.

[4] L. Manuguerra, F. Cappelletti, M. Rossi, and M. Germani, "Design of electric vehicles for Industry 4.0: the case of an autonomous mobile robot," in *Procedia CIRP*, Elsevier, 2023, pp. 980–985. doi: 10.1016/j.procir.2023.05.165.

[5] Y. Dai and H.-J. Lee, "Torque Ripple and Electromagnetic Vibration Suppression by Rotor Notching and Skewing," *Energies (Basel)*, vol. 17, no. 19, p. 4964, 2024, doi: 10.3390/en17194964.

[6] "Harmonic Suppression in Permanent Magnet Synchronous Motor Currents Based on Quasi-Proportional-Resonant Sliding Mode Control." Accessed: Oct. 21, 2025. [Online]. Available: https://www.mdpi.com/2076-3417/14/16/7206?utm_source=chatgpt.com

[7] M. Mehrasa, H. Gholinezhadomran, P. Tarassodi, E. M. G. Rodrigues, and H. Salehfar, "Robust model-based control and stability analysis of PMSM drive with DC-link voltage and parameter variations," *Results in Control and Optimization*, vol. 17, p. 100469, Dec. 2024, doi: 10.1016/J.RICO.2024.100469.

[8] S. Hua *et al.*, "Improved Skew Method in Permanent Magnet Motor with Segmented Rotors for Reducing Cogging Torque," *Progress In Electromagnetics Research C*, vol. 141, pp. 185–193, 2024, doi: 10.2528/PIERC23101906.
[9] P. Yi, W. Zheng, and X. Li, "Overview of Torque Ripple Minimization Methods for Permanent Magnet Synchronous Motors Based on Harmonic Injection," *Chinese Journal of Electrical Engineering*, vol. 10, no. 2, pp. 16–29, 2024, doi: 10.23919/CJEE.2023.000045.
[10] S.-H. Lee, S.-W. Song, I.-J. Yang, J. Lee, and W.-H. Kim, "Optimal Rotor Design for Reducing Electromagnetic Vibration in Traction Motors Based on Numerical Analysis," *Energies (Basel)*, vol. 17, no. 23, p. 6206, 2024, doi: 10.3390/en17236206.
[11] G. V. Research, "Agricultural Robots Market Size, Share & Trends Analysis Report by Type (Automated Harvesting, Automated Irrigation), by Application (Seeding & Planting, Field Farming), by Region, and Segment Forecasts, 2024-2030," *Grand View Research*, 2024, [Online]. Available: https://www.grandviewresearch.com/industry-analysis/agricultural-robots-market
[12] A. Elhaj and A. Mohamed, "Direct voltage MTPA control of interior permanent magnet synchronous motors," *Renewable and Sustainable Energy Reviews*, vol. 133, pp. 110–122, 2025, doi: 10.1016/j.rser.2020.110356.
[13] Z. Yi and W. Wang, "Deep flux weakening control of IPMSM based on d-axis current error integral regulator," *Progress In Electromagnetics Research*, vol. 172, pp. 1–10, 2025, doi: 10.2528/PIER23080101.
[14] Y. Ould Lahoucine and M. Benbouzid, "Line-start permanent magnet synchronous motors: Design and control," *MDPI Energies*, vol. 18, no. 17, p. 4545, 2025, doi: 10.3390/en18174545.
[15] Z. Wu, "Analytical Modeling and Calculation of Electromagnetic Torque of Interior Permanent Magnet Synchronous Motor Considering Ripple Characteristics," 2021. doi: 10.4271/2021-01-0769.
[16] S. Gradev, "Modeling and Control of a Dual-Voltage Synchronous Machine," Technical University of Munich, 2021.
[17] T. Guo, "An IPMSM Control Structure Based on a Model Reference Adaptive Algorithm," *Machines*, vol. 10, no. 7, p. 575, 2022, doi: 10.3390/machines10070575.
[18] A. Elhaj and others, "Direct-voltage MTPA control of interior permanent magnet synchronous motor," *Control Eng Pract*, 2024, doi: 10.1016/j.conengprac.2024.105922.

This page is intentionally left blank